Istraživanja i projektovanja za privredu
ISSN 1451-4117
DOI:10.5937/jaes0-47248
www.engineeringscience.rs

Journal of Applied Engineering Science
Vol. 22, No. 3, 2024
Original Scientific Paper
Paper number: 22(2024)3, 1219, 547-553

NUMERICAL ANALYSIS OF AN AUTOMOTIVE CAGE USED IN THE PERUVIAN MINING SECTOR

Junior V. Angeles-Rocca[1], Carlos A. Alvarado-Silva [2]*, Geraldo César Rosário de Oliveira[3], André Cristiano De Souza[3], Fernando de Azevedo Silva[3]

[1] University Señor de Sipán, Mechanical Electrical Engineering Department, Chiclayo, Peru
[2] Cesar Vallejo University, Mechanical Electrical Engineering Department, Trujillo, Peru
[3] Paulista State University "Júlio de Mesquita Filho", Mechanical Engineering Department, Sao Paulo, Brazil
** calvarados@ucv.edu.pe*

A comparative analysis was conducted between the two structural formats employed in crafting internal roll cages in the Peruvian domestic market (Tubular and Laminar). The aim was to discern the protective effectiveness of each design. The examined cage design pertains to the most prevalent light utility vehicle used within the national mining sector. The computational analysis sought to derive Von Mises forces, resultant deformations, safety factors, and displacement along the applied force direction. This simulation was executed through finite element analysis, incorporating regulations sourced from the International Automobile Federation (FIA) and the Federal Motor Vehicle Safety Standards (FMVSS), which were adapted via analysis of Roll Over Protective Structures (ROPS). The results demonstrate a substantial safety factor in the laminar cage and a lesser concentration of Von Mises stresses in the tubular cage. Nonetheless, both structures experience significant deformations when subjected to lateral loads and at their respective joints. As a conclusion, it can be deduced that both structural configurations adopted in the crafting of interior roll cages adhere to specified standards. Notably, the laminar cage presents aesthetic and mechanical advantages. How-ever, the necessity for experimental testing to comprehend the structure's dynamic behaviour is underscored.

Keywords: finite elements, automotive safety cages, structural deformations, stress analysis

1 INTRODUCTION

Traffic accidents rank among the top ten most common causes of death globally, as reported by [1]. Out of the total 54% of global fatalities in 2016, traffic accidents accounted for 1.4 million deaths. Among these fatalities, 74% were males, with the most heavily impacted age group being the younger population [1].

Since transport accidents (including crashes, detachments, and road overturning) account for an average of ten percent of fatalities within mining operations over the past four years, companies in the mining sector are compelled to procure vehicles equipped with enhanced safety features and better suited for the challenging mine environment. Light trucks are among the favored vehicles for transportation, particularly well-suited for deployment in construction or mining zones. This preference stems partly from their durability and ease of maneuvering within highly hazardous areas. Considering the safety and occupational health regulations prevalent in the mining sector, light transport vehicles are required to be equipped with mandatory safety belts in both the front and rear seats [2].

The regulation does not provide specific details regarding other complementary safety systems. Additional safety measures, such as safety film on windows, roll-over systems, and internal or external protective cages, along with vehicle modifications, are left as choices for enhancement, if they do not compromise the overall vehicle safety [3].

Presently, the application of roll cages has been expanded to encompass light vehicles within the auto-motive fleet. However, the fabrication of these frameworks is still carried out within specialized workshops and through diverse methods. A multitude of roll cage models are available in the market.

In the Peruvian market, two distinct structural types can be discerned: tubular and laminar. The latter is dubbed the "invisible" roll cage due to its characteristic of occupying minimal cabin space. The existence of these alternatives becomes evident through various companies that both vend these products and provide installation services.

Given the two internal anti-roll cage configurations that have been introduced, and considering the absence of regulations governing their implementation, there exists a substantial amount of un-certainty concerning the protective effectiveness of these structures in their distinct formats. Thus, this research project aims to assess this aspect. It is expected that this configuration will exhibit enhanced attributes in mitigating automobile accidents within mining.

2 METHODOLOGY

The methodology for this study was grounded in regulations from the International Automobile Federation (FIA) [4] and the Federal Motor Vehicle Safety Standards (FMVSS), adapted through the analysis of Roll Over Protective Structures (ROPS). FIA regulations provide comprehensive guidelines for roll cages in motorsports, ensuring structural integrity and occupant protection during rollovers. FMVSS 216, which specifies roof crush resistance, ensures that vehicle structures can withstand significant force without collapsing, thereby protecting occupants. This combination of standards offers a robust framework for evaluating the safety of roll cage designs in the mining sector [5].

Furthermore, the study references additional international standards such as ISO 5700 and ISO 3463, which set rigorous global criteria for static and dynamic ROPS tests, respectively. These standards ensure that the roll cage structures meet comprehensive safety benchmarks [6]. By incorporating these well-established regulations and standards, the methodology aligns with globally recognized safety practices, thereby enhancing the credibility and relevance of the analysis. This approach ensures that the roll cage designs are evaluated against the highest safety benchmarks, effectively addressing the protection requirements for light utility vehicles in the mining sector [7].

The structure featuring the concealed internal anti-roll cage was constructed using ballistic steel, utilizing a 6 mm thick laminar profile (AR500). This information was sourced from official websites of suppliers and installers specializing in these structures, with a strong emphasis on vehicle armoring and overall security. For the other examined structure (tubular cage), a tubular profile made of ASTM-A36 steel with a diameter of 45 mm and a thickness of 2.5 mm was employed. The properties and general characteristics are shown in Table 1 according to [8].

Table 1. Mechanical properties of study materials.

Material property	AR-500	ASTM-A36	Unit
Modulus of elasticity	20500	200000	N/mm^2
Poisson's coefficient	0.26	0.26	-
Shear module	357000	79300	N/mm^2
Mass density	7850	7850	Kg/m3
Tensile strength	1550	400	N/mm^2
Yield strength	1200	250	N/mm^2
Material property	AR-500	ASTM-A36	Unit

2.1.1 Structural geometry of roll cage

The configuration of the internal roll cage is directly influenced by the interior layout of the cabin where it will be installed [9]. Keeping this factor in mind along with the chosen chassis model (Pick-up), it was deemed appropriate to designate the most frequently employed light vehicle model within the Peruvian mining context. Subsequently, a 3D model of the respective internal roll cage was developed. Fig. 1 illustrates the geometry, positioning, and considerations that were factored in while creating the structure for the two examined scenarios.

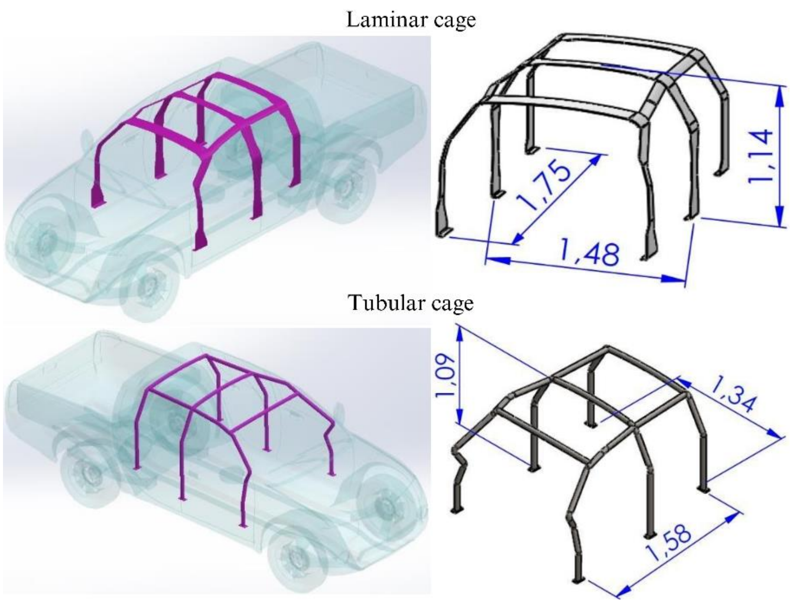

Fig. 1. Vehicle cage frame geometry details

The geometry of the internal laminar anti-roll cage aligns with the bodywork's surface, attaching itself through welding. This design choice prevents interference with other protective systems while offering greater flexibility to cover critical zones [10]. The cage primarily employs rectangular profile sheets for the body structure, resulting in a 72 kg mass. This configuration creates an imperceptible shield that occupies no internal space, and it can be concealed by the vehicle's upholstery to maintain its aesthetic appeal.

On the other hand, the internal tubular anti-roll cage's geometry follows the cabin's surface, connecting to the chassis to ensure no compromise with other safety mechanisms like seat belts and air-bags [5]. Comprising a central main arch, a rear arch, and two semi-lateral arches, this design includes a supporting beam before reaching the windshield. The overall mass of this structure is 46 kg.

2.1.2 Initial condition

Presently in Peru, there exists no regulation outlining the fundamental parameters that these vehicular accessories (anti-vehicle cages) should adhere to. The only stipulation is that their installation should not pose any risk to the driver or other passengers [11]. Nevertheless, in the realm of competitive and tourist vehicles, there exists an extensive checklist of prerequisites for these passive safety systems. This checklist standardizes the forces they must withstand and specifies the conditions under which deformation is acceptable.

As previously noted, this research project will utilize static loads as prescribed by regulations [4] and [5] and detailed in Fig. 2.

Load on the center bar:	
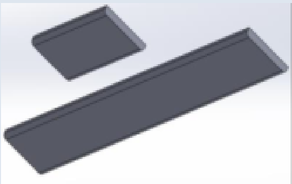	75 x(W Vehicular + 150Kg) N. Maximum permissible deformation of 50 mm in the direction of the force. To distribute the load, a rigid rectangular geometry of the following dimensions is implemented: Length: Width of the main arch + 100 mm, Width: 250 ± 50 mm, Thickness: 40 mm.
Load on frontal bar:	
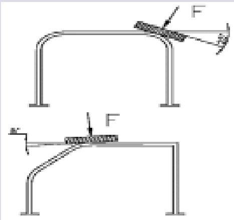 Front and side view.	35 x(Vehicle W + 150 Kg) N. The load distributor will have the following dimensions: Length: 450 ± 50 mm, Width: 250 ± 50 mm, Thickness: 40 mm. The distributor will be positioned as follows: Front tilt: 5°, Lateral tilt: 25°.

Fig. 2. Static loads requested [4,5]

It's important to note that the applied forces are significantly exaggerated to ensure the physical safety of the occupants. This exaggeration is necessary because this regulation pertains to vehicles that operate at speeds considerably greater than what is typical within the Peruvian automotive fleet. The vehicle's specifications are as follows: length = 5.26 m; height = 1.86 m; width = 1.835 m; weight (W) = 2705 kg.

2.1.3 Static analysis according to FIA regulations

To perform the analytical and numerical calculations of the forces that the roll cages need to endure in order to be deemed acceptable, the parameters specified by [4] and [5] for the method and positioning of loading will be employed.

Central bar load: The load in Newtons assigned for this simulation derives from the vehicle's weight (W), computed using the equation for the Central bar load depicted in Fig. 2, amounting to 202,875 KN. Initially, the assembly to be simulated is established, representing the roll cage along-side a block positioned on the central arch to direct the force that the structure will withstand.

To adequately support the block, a channel was created and positioned on the arch with the necessary positional alignment. The upcoming simulation will involve a three-dimensional static analysis [7]. The existing connections within the assembly are defined as "rigid joints" between the force block and the primary beam constituting the central arch of the structure. By designating this as a rigid joint, it enables it to act as a unified element, uniformly distributing the force—a prerequisite for the software's accurate interpretation of the calculation [8]. In the fixation segment, the mobility of the structure's legs is constrained. These joints are configured as fixed geometries, and for each unbound joint, its rotation and translation are limited, simulating attachment to the vehicle chassis.

A vertical load of 202,875 kN, equivalent to 75 times the vehicle's gross weight, is applied onto the block. The mesh employed incorporates a blend of curvature-based meshing, with a maximum element size of 15mm and a minimum of 5mm.

Front bar load: The International Automobile Federation [4] dictates that the load ap-plied to the front bar of the vehicle must adhere to a specific angle of inclination. This angle is crucial for simulating a side impact during a rollover. Additionally, this force is directly correlated with the vehicle's weight, as indicated by the Front bar load equation in Fig. 2, which amounts to 94,675 KN. The defined assembly for simulation represents the roll cage with a block in the front arch. The placement of the block follows the guidelines outlined in the FIA regulations, with a lateral inclination of 25° and a frontal inclination of 5°. This ensures the proper channeling of force. The upcoming simulation will involve a three-dimensional static analysis. The existing connections within the assembly are defined as rigid connections [9], linking the force block with the frontal-lateral beam that comprises the anti-roll cage. In the fastening segment, the mobility of the structure's legs is cur-tailed, establishing them as fixed geometries. Each unrestricted joint is singled out, with its rotation and translation restricted to simulate attachment to the vehicle chassis.

A normal force is applied to the external face of the block. For this simulation, a force of 94,675 kN is utilized, equivalent to 35 times the vehicle's gross weight. The mesh employed incorporates a combination of curvature-based meshing, featuring a maximum element size of 15 mm and a mini-mum of 5 mm.

Fig. 3 displays the static loads and constraints for both scenarios: Fixed geometry signifies the rigid connection of the cage to the chassis. Sliding roller: This will simulate the attachment of the laminar profile to the bodywork through welding. This mode of fastening will restrict the lateral movement of the structure, replicating its behavior in real-world conditions as it directly links to the vehicle frame.

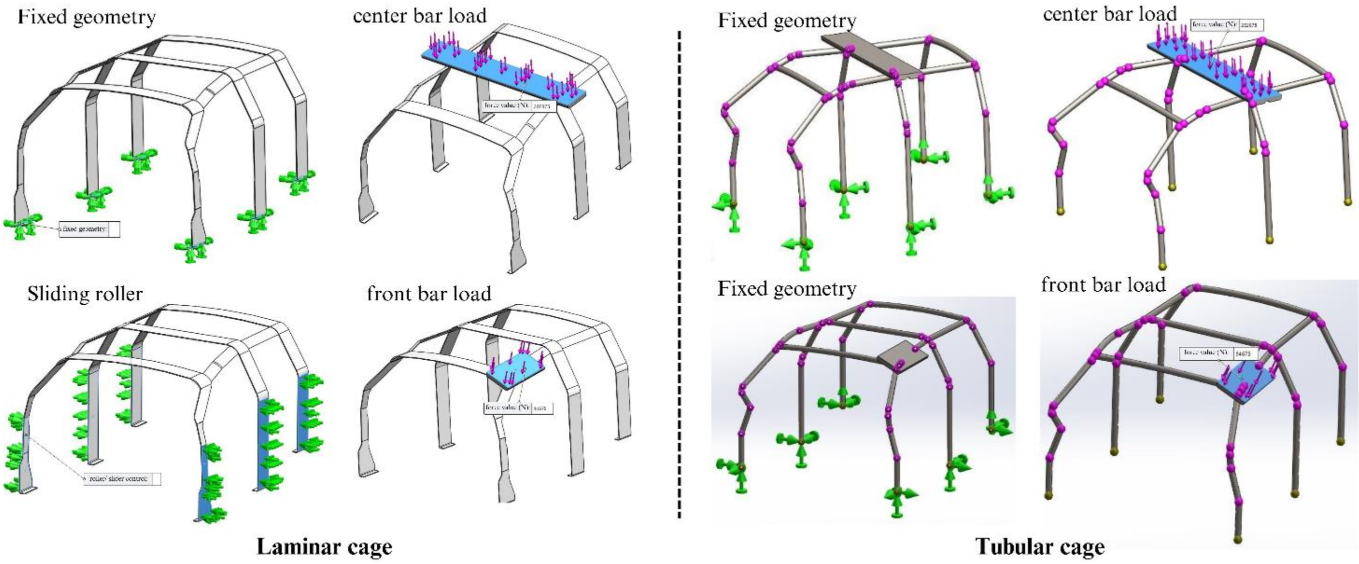

Fig. 3. Static loads and restrictions in both cases

The acting force on the system has the following impacts on the structure:

Von Mises stress: Von Mises stress amalgamates all principal stresses within the structure and serves to evaluate its capacity to withstand plastic deformation [12]. This outcome facilitates the assessment of areas where the structure's inertia should be augmented, necessitating modifications to the geometric parameters of the cage.

Resulting displacements: The applied force induces deformations within the structure, consequently leading to displacements across various sections of the system. Displacements can be quantified in terms of movement or deviation from the initial position. As per [13], the displacement attributed to the loading must not surpass 40 mm.

Safety factor: This indicator gauges the proximity of Von Mises stresses to the material's elastic limit. The safety factor is computed by dividing the material's elastic limit by the resultant Von Mis-es stress. A low safety factor (approaching 1) signifies a nearness to the material's strength limit, implying potential failures or excessive deformations. According to [14], the anticipated value stands at 2.

Deformation in the direction of the force: This parameter quantifies the proportional alteration in the shape or dimensions of a material in relation to its initial state. This measurement offers insights into the degree of deformation within the cage and the material's reaction to the applied load [15].

3 RESULTS

Based on the outcomes presented in Fig. 4, 5, and 6, it becomes apparent that the tubular structure dissipates stresses more effectively. This is evident through a reduced concentration of Von Mises stresses in comparison to the laminar structure. This contrast can be attributed to the cylindrical geometry of the structure, which imparts enhanced structural rigidity to the vehicle cabin.

Conversely, the laminar structure serves as supplementary reinforcement to the existing framework. However, its contribution to structural integrity is minimal upon analysis. In terms of resulting deformation, the laminar protective cage displayed a higher degree of deformation, particularly concerning the frontal bar. The safety factor is intrinsically linked to material properties; thus, for the laminar profile, it is advisable to substitute the proposed material with a stronger alternative.

The displacement along the force application direction exhibits a greater magnitude in the laminar structure. While still within the range of the American standard FMVSS-216, it surpasses the limits stipulated by [6].

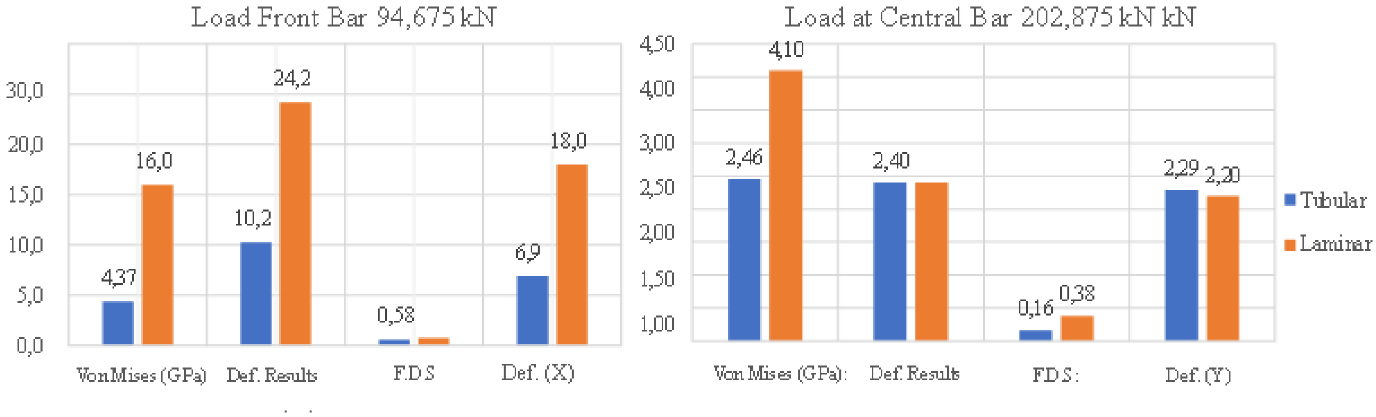

Fig. 4. Results due to loading in the center bar and in front bar

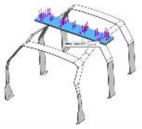 **Load in central bar**		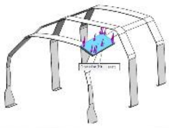 **Load in frontal bar**	
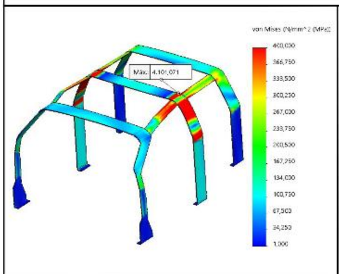	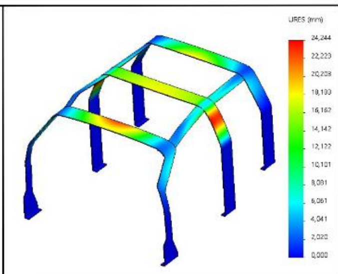	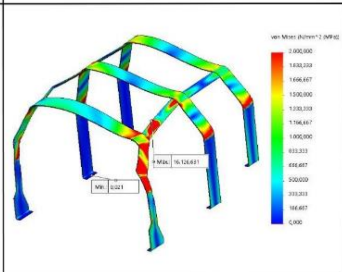	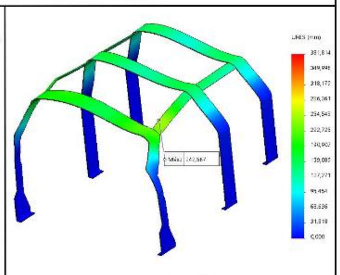
Von Misses stress: The stress is distributed to sides of the cage, showing in the red areas around 4101.07 MPa.	**Resulting displacements:** The resulting deformation obteined after the simulation shows a maximum of 24 mm.	**Von Misses stress:** MAximum stress in the contact area of 16000 MPa.	**Resulting displacements:** The deformation calculated in simulation is approximately 24.2 cm.
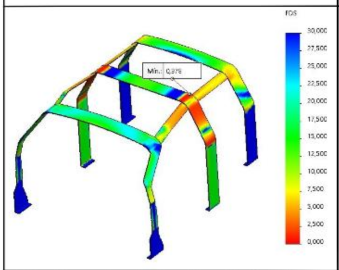	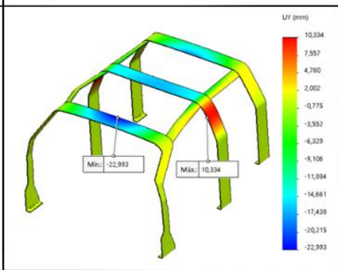	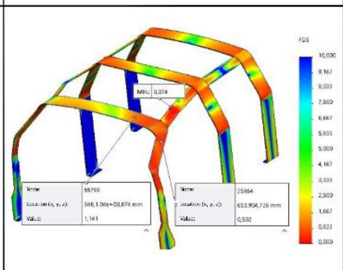	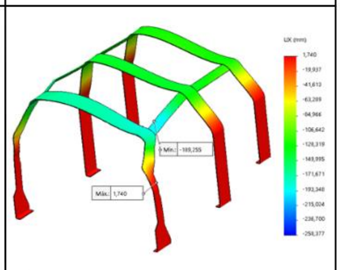
Safety factor: The color chart shows the dispersion of the safety factor throughout the structure with a minimum value of 0.378 in the critical zone of the structure	**Deformation in the force (Y) direction:** The deformation in the direction of the applied force shows a displacement of 22 mm in negative Y, projected on the front bar.	**Safety factor:** Minimum safety factor in the area of stress concentration is 0.074.	**Deformation in the force (X) direction:** A negative x displacement of 18 cm can be seen.

Fig. 5. Results in laminar cage

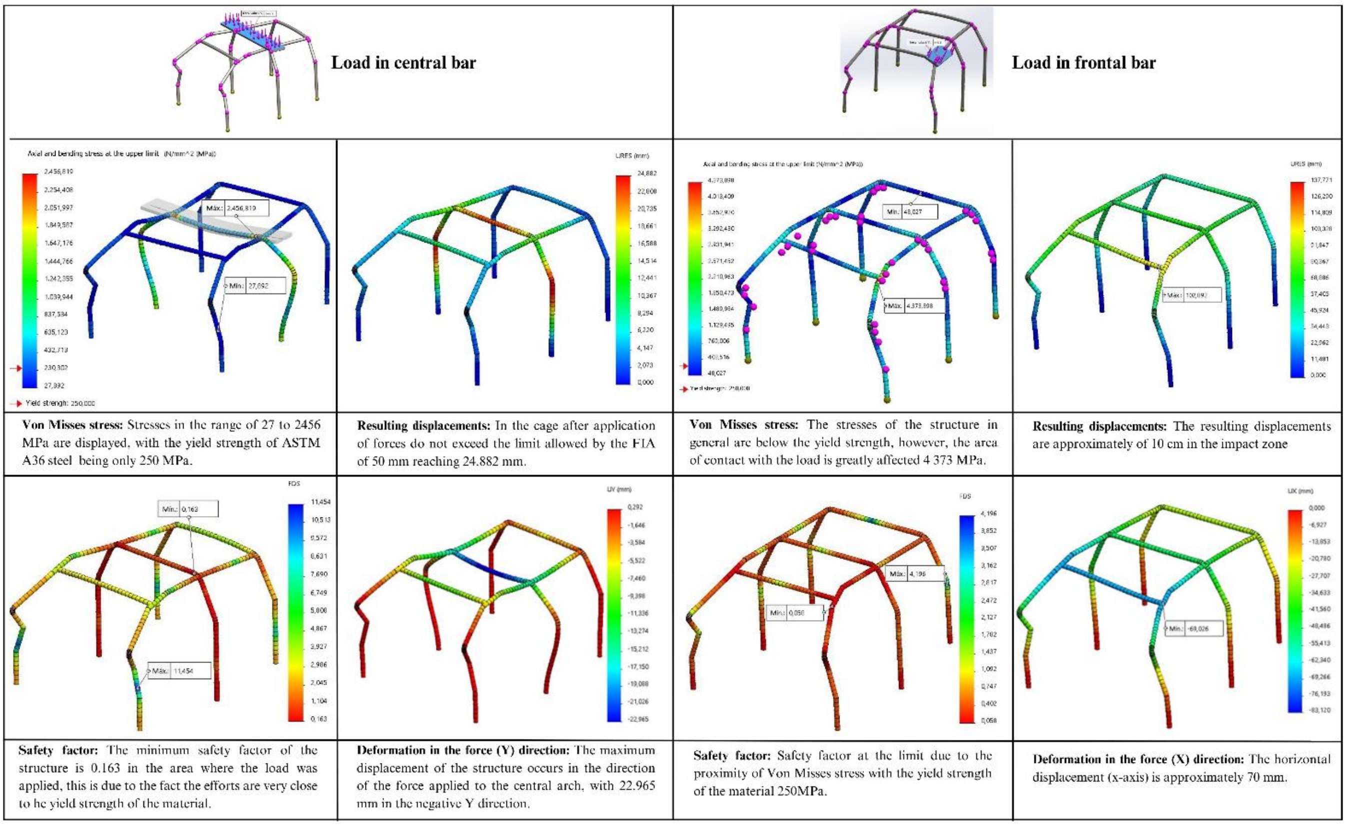

Fig. 6. Results in tubular cage

4 CONCLUSIONS

The conducted analytical studies adhered to rollover conditions, encompassing vertical and side impacts while taking into consideration the vehicle's weight. This computational approach offers cost savings as it yields results without necessitating destructive tests on the vehicles. Within the finite element simulation process, factors such as maximum Von Mises stresses, resultant deformation, safety factors, and the utmost displacement along the force application direction were all considered.

Deformations manifest with lesser intensity in the tubular cage, reflecting the cylindrical geometry and the associated greater inertia intrinsic to its structural profile. Nonetheless, this doesn't inherently grant an advantage over the laminar structure. The laminar configuration might be better suited for the programmed deformation of the vehicle, suggesting a potential enhancement for the chassis structure. However, to increase the safety factor, the utilization of a stronger material like carbon fiber composites becomes necessary.

The utilization of the laminar profile holds the advantage of being inconspicuous within the cabin while offering additional reinforcement to the preexisting framework. Nevertheless, it doesn't independently bestow a greater level of structural integrity when subjected to analysis.

5 REFERENCES

[1] Organización Mundial de la Salud. Un reporte sobre la salud, from http://www.who.int/es/news-room/fact-sheets/detail/road-traffic-injuries, accessed on 2023-12-13.

[2] Ministerio de Transportes y Comunicaciones. Ley General de Transporte y Tránsito Terrestre - N° 27181, from https://www.gob.pe/institucion/congreso-de-la-republica/normas-legales/9868-27181, accessed on 2012-11-21.

[3] Ministerio de Transportes y Comunicaciones. Reglamento Nacional de Vehículos - Decreto Supremo N 058-2003-MTC, from https://www.gob.pe/institucion/mtc/normas-legales/10013-058-2003-mtc, accessed on 2003-10-07.

[4] Federation Internationale De l' Automobile. APPENDIX J – ARTICLE 253 "Safety Equipment for Cars of Group", from https://www.fia.com/sites/default/files/253_2023.pdf, accessed on 2022-12-09.

[5] Federation Internationale De l' Automobile. 2021 Homologation Regulations for Safety Cages, from https://storage-aso.lequipe.fr/ASO/motorSports_ccr/reglement-d-homologation.pdf, accessed on 2021-06-14.

[6] Lewandowski, J. (2006). Federal Motor Vehicle Safety Standard (FMVSS) 208 – Occupant Crash Protection: Right Front Passenger Test Methodologies. SAE 2006 World Congress & Exhibition, p. 1-10, DOI:10.4271/2006-01-0720.

[7] Tobón, C., Patiño, I., Lemmel, K. (2018). Análisis por elementos finitos del desempeño estructural de jaula de seguridad para vehículo Renault Logan bajo normatividad FIA. Revista CINTEX, vol. 23, no. 2, 35-53, DOI: 10.33131/24222208.312.

[8] Fateh, A., Hejazi, F., Jaafar, M. S., Abd Karim, I. (2016). Numerical and experimental evaluation of a developed nonlinear curved spring element under compression force. Journal of Constructional Steel Research, vol. 117, no. 2, 115-125, DOI: 10.1016/j.jcsr.2015.10.011.

[9] Köhn, A., de Azevedo, F. (2020). A numerical and analytical study of the stress field generated by the contact between a rail and a wheel. SN Applied Sciences, vol. 2, no. 6, 1252, DOI: 10.1007/s42452-020-3044-1.

[10] Alvarado-Silva, C. A., Rosario, G, Gamarra-Rosado, V., de Azevedo, F. (2022). A Polynomial Equation Model for Fatigue Crack Propagation in an Aeronautical Steel Material. Materials Science Forum, vol. 1053, 212–217. DOI: 10.4028/p-7j8ye8.

[11] Putini, E., de Azevedo, F. (2018). Fatigue life estimation in a hydrogenerator rotor with cracks using the finite element method. Journal of the Brazilian Society of Mechanical Sciences and Engineering, vol. 40, no. 9, 1-15, DOI: 10.1007/s40430-018-1340-0.

[12] Marques, B., Marques, T., de Azevedo, F., Cândido, G., Rezende, M. (2023). Failure criteria assessment of carbon/epoxy laminate under tensile loads using finite element method: Validation with experimental tests and fractographic analysis. Mechanics of Advanced Materials and Structures, vol. 30, no. 6, 1274 – 1283, DOI: 10.1080/15376494.2022.2029984.

[13] Naima, J., Nissrine, M., Mohammed, R., Benaissa, El Fahime. (2023). Numerical investigation of premature fatigue of highspeed train wheels in presence of facets defect with case study. Journal of Applied Engineering Science, vol. 21, no. 4, 1062-1073, DOI: 10.5937/jaes0-43734.

[14] Nicola, L., Cima, M. (2024). Development of a fem procedure for evaluating the pressure profile in the industrial wheel and fatigue strength analyses. Journal of Applied Engineering Science, vol. 22, no. 1, 171-183, DOI: 10.5937/jaes0-48184

[15] Corda, J., Chethan, K., Satish, B., Shetty, S., Shyamasunder, N., Zuber, M. (2023). Damage fatigue life evaluation of different hip implant designs using finite element analysis. Journal of Applied Engineering Science, vol. 21, no. 3,896–907, DOI: 10.5937/jaes0-44094.

Paper submitted: 21.10.2023.
Paper accepted: 09.07.2024.